Optics Communications 284 (2011) 777–781

Contents lists available at ScienceDirect

Optics Communications

journal homepage: www.elsevier.com/locate/optcom

High fill-factor multilevel Fresnel zone plate arrays by femtosecond laser direct writing

Li-Gang Niu, Dian Wang, Tong Jiang, Si-Zhu Wu, Ai-Wu Li *, Jun-Feng Song *

State Key Laboratory on Integrated Optoelectronics, College of Electronic Science and Engineering, Jilin University, 2699 Qianjin Street, Changchun 130012, China

ARTICLE INFO

Article history:
Received 17 June 2010
Received in revised form 23 September 2010
Accepted 27 September 2010

ABSTRACT

Fresnel zone plate arrays (FZPAs), as a kind of an important integrated micro-optical device, have attracted great attention. However, the fill factor of present FZPAs by femtosecond technology is a little low, which leads to serious light loss and low signal-to-noise. Here we reported high fill-factor square and hexagonal FZPAs by femtosecond laser two-photon polymerization of the resin SU-8. Their optical focusing and imaging properties showed the high uniformity and high fidelity of these FZPAs. Moreover, 100% fill-factor FZPAs were demonstrated by optimal theoretical design and experimental parameters. With this high quality FZPAs, clear imaging "F" was obtained. At last, high-level phase type FZPAs were prepared to further enhance the diffractive efficiency to as much as 75%.

1. Introduction

With the trend of device miniaturization and optical device integration, the field of diffractive micro-optical devices has attracted extensive attention over the past decade due to their small volume, light weight, flexible design and batch production [1]. Fresnel zone plate arrays (FZPAs) with diameters about several micrometers, as a kind of focusing and imaging micro-optical device, are key components for various micro-optical applications, particularly in laser shaping, optical neural network, optical interconnection [2], liquid-crystal display [3], and confocal microscopy [4]. A variety of techniques have been developed to fabricate Fresnel zone plates and their arrays, such as focused ion beam etching [5], electrochemical micromachine [6], photolithography [7] and so on. However, these methods are usually complex multistep processes. Moreover, these methods are difficult to integrate various complex 3D micro-optical devices [8–10] towards more compact and integrated photonic circuits.

Femtosecond direct writing technology [11–24] has been recently considered as a promising approach to integrate arbitrary 3D micro-optical devices towards integrated optical circuits. Various micro-optical devices, such as 3D photonic crystals [11–13], bandpass filters [14], and Dammann grating [15] have been realized. Recently, many researchers also have paid great attentions to high quality Fresnel zone plate arrays. For instance, Huang et al. [25] firstly demonstrated amplitude-type FZP by two-photon polymerization of the commercial photoresist SCR500. Sun et al. [26] fabricated phase type two-, four-, and eight-level FZP with level thicknesses of 475, 238, and 119 nm to dramatically improve the diffractive efficiency. Mizoshiri et al. [27] firstly reported SiO_2 FZPAs by combining femtosecond microfabrication with plasma etching. Although the great progress has been made towards high quality FZPAs, the present FZPAs are of low fill factor (~50%), which leads to serious light loss and lower signal-to-noise ratio. In practical applications, high fill factor (>90%), especially 100% fill factor, is highly demanded.

In this paper, we reported close-packed square and hexagonal FZPAs by femtosecond laser direct writing with nanoscale precision. Moreover, by optimal design model and experimental parameters, 100% fill-factor FZPAs were realized. With this high quality FZPAs, sharp focusing and clear imaging were demonstrated. Finally, high-level phase type FZPAs were prepared to further enhance the diffractive efficiency.

2. Experimental setup

A schematic diagram of the experiment is shown in Fig. 1. A Ti–sapphire femtosecond laser (from Tsunami, Spectra Physics) was used. It generated laser pulses at 790 nm mode-locked with a duration of 120 fs at a repetition rate of 80 MHz, which was tightly focused into the resin by a high numerical aperture (NA = 1.35, oil immersion) objective lens. The laser spot was scanned on the focal plane by a two-galvano-mirror set and along the optical axis by a piezo stage, both controlled by a computer so as to make the computer patterns be faithfully converted into a practical structure. We adopted an annular scanning mode [8] to obtain better optical property because the subzones of the FZPAs were all circular. The SU-8 films were prepared by spin-coating on a cover slip which had been cleaned with acetone and absolute ethanol. After a soft-bake step by 3 min at 65 °C and

* Corresponding author.
E-mail address: songjf@jlu.edu.cn (J.-F. Song).

0030-4018/$ – see front matter
doi:10.1016/j.optcom.2010.09.066

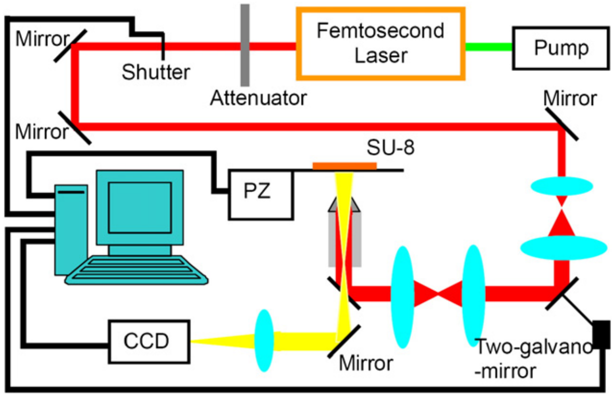

Fig. 1. A schematic diagram of the femtosecond microfabrication system.

30 min at 95 °C, the solvent evaporated and a 10 μm thick film formed. Under irradiation by femtosecond laser, the photoinitiator generated spatial distribution acid. In a post-exposure bake from 65 °C to 95 °C for 10 min, the latent structure was converted into a cross-linked solid skeleton by the chain propagation of the crosslinking process. Then, the sample was developed in the SU-8 developer (1-methoxy-2-propylacetate) for 30 min, leading to a positive image of the scanned FZPAs.

3. Results and discussion

3.1. Square Fresnel zone plates

Fig. 2(a) shows bird-eye view scanning electron microscope (SEM) images of square Fresnel zone plate arrays fabricated by two-photon photopolymerization of the commercial epoxy-based negative resin SU-8 along the designed model [Fig. 2(b)]. The optimal laser power was about 6 mW and the exposure time was chosen as 1 ms in order to realize 100 nm-single voxel. The resin has a high transmittance for light from the visible to the near infrared wavelengths, low polymer volume shrinkage, good mechanical properties (Young's modulus, E~4–5 GPa and biaxial modulus of elasticity~5.2 GPa) and high thermal stability (the degradation temperature ~380 °C), making it suitable for micro-optical component fabrication. The Fresnel zone plate consists of a series of concentric zones with radii defined by

$$r_m^2 + f^2 = (f + m\lambda/2)^2$$
$$r_m = \sqrt{m\lambda f + (m\lambda/2)^2} \approx \sqrt{m\lambda f} \quad (m\lambda << f) \qquad (1)$$

where f is the focal length, and r_m is the outer radius of the mth zone. The diameter of every FZP is about 27 μm and the refractive index of the SU-8 resin is 1.56. The thickness of the FZPAs was designed as 475 nm, in order to induce the phase change of π at a wavelength of 532 nm. To characterize its optical properties, an optical evaluation system consisting of a 3D positioning stage, a 60× objective lens, and a CCD (charge coupled devices) camera was set up, as shown in Fig. 3(b). The diameter of the cross-section of the incident output laser beam was about 1 mm, which was much larger than the size of the FZPAs. The incident light was firstly focused by the Fresnel zone plate, and the focal spots were amplified by a 60× objective and imaged into a detector (C30724, Hofoo, Co. Ltd.). The iris placed in front of the detector blocked unwanted light. The observed focal spot arrays were shown in Fig. 2(c). During the fabrication process, several fabrication errors, such as the stability of the laser intensity, sidewall errors, etc., probably affected the optical properties of FZPAs. Besides, they have a significant impact on the uniformity of the focal spot intensity, which is an important criterion for evaluating FZPAs. For an intuitional view, the uniformity was manifested as Fig. 2(d). Each peak indicated the intensity of its corresponding spot along the dashed lines in Fig. 2(c). From the curve of Fig. 2(d), we could see that the intensity of these focal spots was uniform.

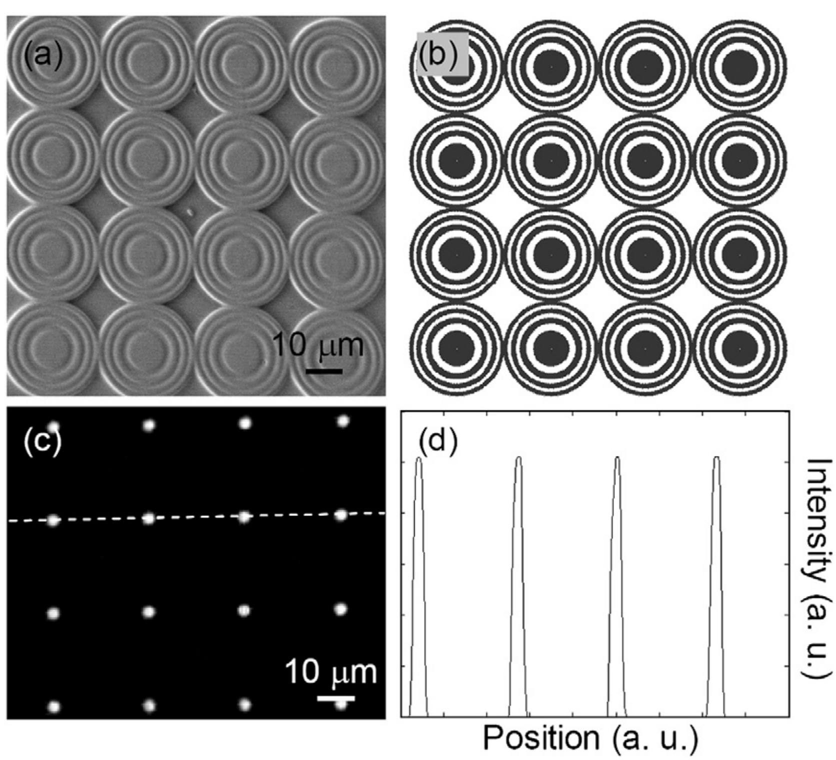

Fig. 2. Square Fresnel zone plate arrays fabricated via two-photon photopolymerization of the commercial epoxy-based negative resin SU-8. (a) Bird-view scanning electron microscope image of square FZPAs. (b) The designed model of FZPAs. (c) The observed focal spot arrays of FZPAs under light illumination. (d) The intensity distribution of the focal spot arrays, showing the uniformity of FZPAs.

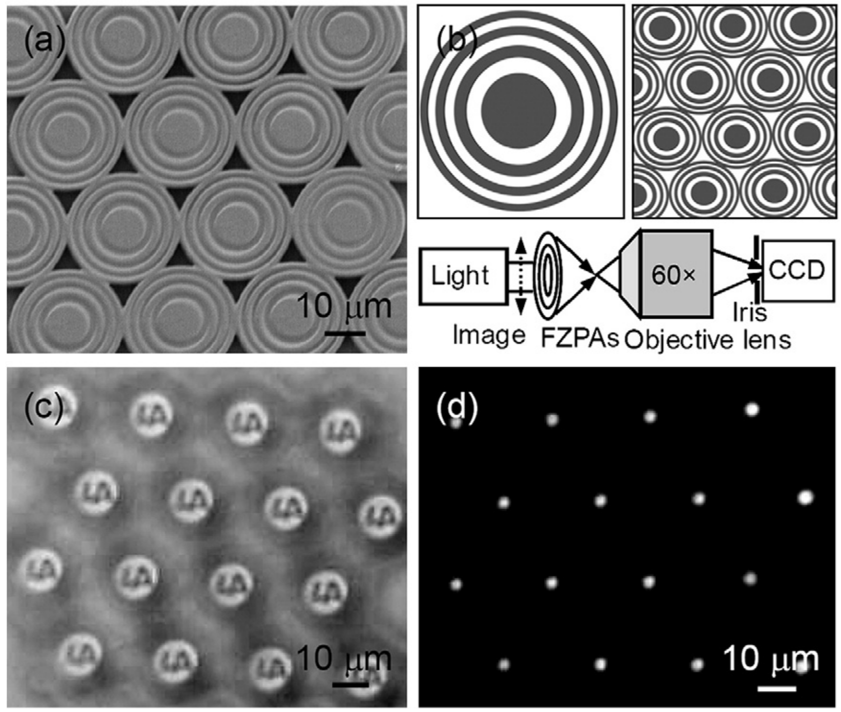

Fig. 3. High quality hexagonal Fresnel zone plates by femtosecond laser direct writing and their optical properties. (a) Bird-view SEM image of hexagonal FZPAs. (b) The solid model of FZP, 3D geometry of close-packed hexagonal FZPAs, and their optical characterization system. (c) The real image of the two letters "LA", the abbreviation of "laboratory". (d) The focal spot of hexagonal FZPAs.

The focal length of FZPAs is deduced along Eq. (2):

$$f = r_1^2 / \lambda. \tag{2}$$

Given $r_1 = 5.1$ μm, we get $f = 49$ μm, which agrees well with the measured value 55 μm.

3.2. Hexagonal Fresnel zone plates

The fill factor defined as the percentage of FZPAs area to the total area is about 78.5% for square FZPAs. Hexagonal FZPAs are another kind of FZPAs arrangement and their fill factor reaches as much as 91%. A hexagonal FZPA was designed by computer program. The solid model of an FZP and the 3D geometry of close-packed hexagonal FZPAs are shown in Fig. 3(b). According to the designed model, hexagonal FZPAs were precisely realized by point-to-point scanning, as shown in Fig. 3(a). According to AFM measurement, the FZPA had a smooth surface with a surface roughness less than 8 nm, which ensures the high surface quality and excellent optical properties of the FZPAs. Fig. 3(d) showed that a hexagonal array of uniform and sharp focal spots was observed behind the microscopic objective lens when the FZPAs were illuminated by 532 nm-wavelength light. To further investigate the optical performance of FZPAs, two letters "LA", the abbreviation of "laboratory", were placed at the front of FZPAs, and the image was magnified by objective lens and received by a CCD, as shown in Fig. 3(c). The image of micro-letters "LA" was clearly observed, which showed excellent focusing and imaging ability of the high quality FZPAs.

3.3. 100% fill-factor Fresnel zone plates

To further enhance the light utilization, 100% fill-factor FZPAs were designed by optimal computer programs [Fig. 4(b)] and precisely prepared by femtosecond laser two-photon polymerization. As can be seen from Fig. 4(a), all the FZPs are close-packed and there is no gap between these adjacent FZPs. It is well known that 100% fill-factor FZPAs are expected to ultimately utilize the entire incident light and enhance the image brightness of liquid-crystal displays and raise the out-coupling efficiency in light-emission diodes. Moreover, with this high fill-factor FZPAs, clear image "F" was demonstrated, as shown in Fig. 4(d).

Besides fill factor, diffractive efficiency, defined as the ratio of the intensity of diffracted light at the focal spot to the intensity of incident light into the zone plate, is another important parameter for FZPAs. The measured diffractive efficiency by a semiconductor laser with a wavelength of 532 nm was 33.7%, 35%, and 33% for square, hexagonal and 100% fill-factor hexagonal FZPAs, which was very close to the theoretical maximal 40.5% of two-level FZP. The achievement of such high diffractive efficiency may be attributed to the high precision of femtosecond laser technology when the experimental parameters were optimized.

3.4. Multilevel phase type Fresnel zone plates

To enhance the diffractive efficiency of the FZPAs, we tried to design high-level phase type FZPAs. For an N-level FZP, its diffractive efficiency is [23]:

$$\eta_{KNF}(N) = \frac{\sin^2(\pi / N)}{(\pi / N)^2} = \sin c^2(1 / N). \tag{3}$$

For $N = 2$, and $N = 4$, the theoretical efficiency is 40.5%, and 81.0%, respectively. The layer thickness is defined by $d = \lambda / N(n-1)$, so their subzone layer thickness is 475 nm and 237.5 nm, respectively, in order to induce the phase change of π and π/2 at each subzone, respectively. Shown in Figs. 5(a) and (c) are the bird-view and locally magnified SEM images of four-level square FZPAs. From the magnified SEM image, we clearly see that every zone is divided into four subzones. The bright focal spot arrays are shown in Fig. 5(b). The diffractive efficiency reached as much as 75%. The fill factor for the square four-level FZPAs is about 78.5%. Besides square FZPAs, high

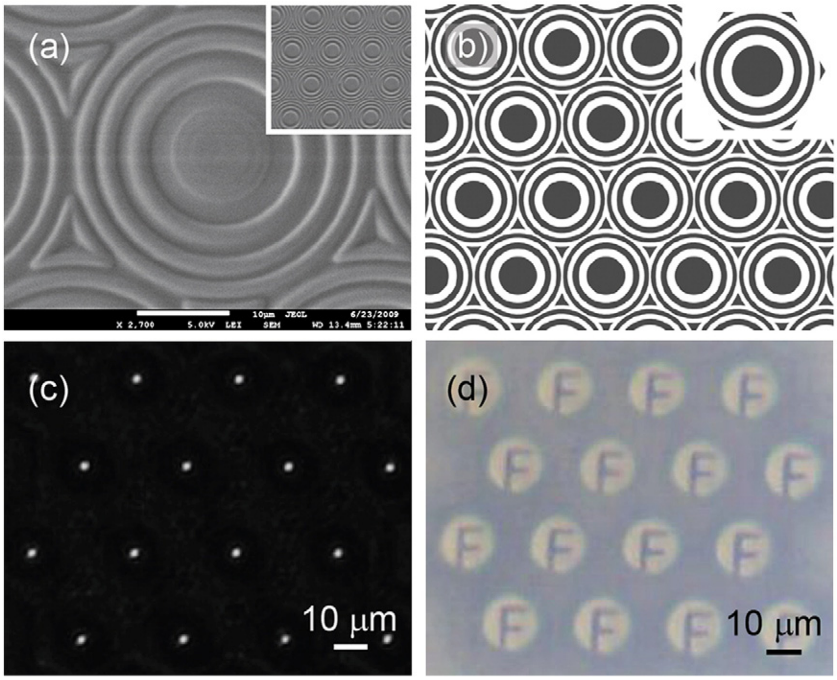

Fig. 4. 100% fill-factor FZPAs prepared by two-photon point-to-point writing method. (a) Bird-view SEM image of 100% fill-factor FZPAs. The inset is the whole SEM image. (b) The designed model of 100% fill-factor FZPAs. The inset is the model of an FZP unit. (c) The focal spot array. (d) Clear image "F" formed by this high fill-factor FZPAs.

quality four-level hexagonal FZPAs with 91% fill factor were realized by direct laser writing, as shown in Fig. 5(d). All these FZPs were close-packed to realize high fill factor.

4. Conclusion

Close-packed square and hexagonal FZPAs were realized by femtosecond laser two-photon polymerization. Their optical properties were systemically investigated. Moreover, by optimizing the calculation design and experimental parameters, 100% fill-factor FZPAs were demonstrated. With this high quality FZPAs, clear image "F" was obtained. Finally, high-level phase type FZPAs were prepared to enhance the diffractive efficiency to as much as 75%, which is close to the theoretical maximal. This work shows not only the feasibility of the combination of the high fill-factor and multilevel structure but also excellent flexibility and high accuracy of the femtosecond laser

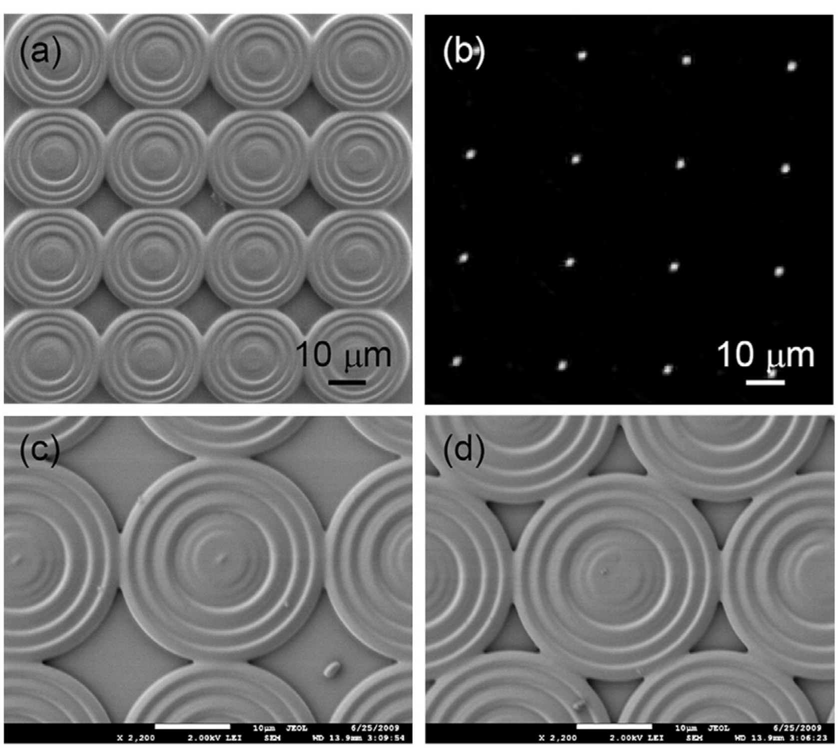

Fig. 5. High-level phase type FZPAs fabricated by one-step direct writing. (a) and (c) are the bird-view and locally magnified SEM images of four-level square FZPAs. Every zone was divided into four subzones. (b) The bright focal spot arrays. (d) Bird-view SEM image of high quality four-level hexagonal FZPAs.

direct writing technology. The high fill-factor FZPAs with improved optical performances may find broader applications in optical communication, optical interconnections, and integrated optical circuits.

This work was supported by the NSFC under grant no. 90923037. The authors appreciate Prof. Hong-Bo Sun, College of Electronic Science and Engineering, Jilin University, for his valuable discussion about this work.

References

[1] M.C. Hutley (Ed.), Microlens arrays: proceeding of a one day seminar, Inst. of Physics Pub. Inc, Teddington, 1991.
[2] Y.A. Peter, H.P. Herzig, R. Dandliker, IEEE J. Quantum Electron. 8 (2002) 46.
[3] Y. Huang, D. Shieh, S. Wu, Appl. Opt. 43 (2004) 3656.
[4] M. Eisner, N. Lindlein, J. Schwider, Opt. Lett. 23 (1998) 748.
[5] M.K. Lee, K.K. Kuo, Appl. Phys. Lett. 91 (2007) 05111.
[6] L. Zhang, X.Z. Ma, J.L. Zhuang, C.K. Qiu, C.L. Du, J. Tang, Z.W. Tian, Adv. Mater. 19 (2007) 3912.
[7] J. Jahns, S.J. Walker, Appl. Opt. 29 (1990) 931.
[8] D. Wu, L.G. Niu, Q.D. Chen, R. Wang, H.B. Sun, Opt. Lett. 33 (2008) 2913.
[9] X.Z. Dong, Q. Ya, X.Z. Sheng, Z.Y. Li, Z.S. Zhao, X.M. Duan, Appl. Phys. Lett. 92 (2008) 231103.
[10] D. Wu, Q.D. Chen, L.G. Niu, J. Jiao, H. Xia, J.F. Song, H.B. Sun, IEEE Photon. Technol. Lett. 21 (2009) 1535.
[11] M. Deubel, V. Freymann, M. Wegener, S. Pereira, K. Busch, C.M. Soukoulis, Nat. Mater. 3 (2004) 444.
[12] D. Wu, S.Z. Wu, L.G. Niu, Q.D. Chen, R. Wang, J.F. Song, H.H. Fang, H.B. Sun, Appl. Phys. Lett. 97 (2010) 0371109.
[13] H.B. Sun, S. Matsuo, H. Misawa, Appl. Phys. Lett. 74 (1999) 786.
[14] M. Li, K. Mori, M. Ishizuka, X.B. Liu, Y. Sugimot, N. Ikeda, K. Asakawa, Appl. Phys. Lett. 83 (2003) 216.
[15] Q.D. Chen, X.F. Lin, L.G. Niu, D. Wu, W.Q. Wang, H.B. Sun, Opt. Lett. 33 (2008) 2559.
[16] D.F. Tan, Y. Li, F.J. Qi, H. Yang, Q.H. Gong, X.Z. Dong, X.M. Duan, Appl. Phys. Lett. 90 (2007) 071106.
[17] S. Kawata, H.B. Sun, T. Tanaka, K. Takada, Nature 412 (2001) 697.
[18] K. Seet, V. Mizeikis, S. Matsuo, S. Juodkazis, H. Misawa, Adv. Mater. 17 (2005) 541.
[19] D. Wu, Q.D. Chen, L.G. Niu, J. Wang, R. Wang, H. Xia, H.B. Sun, Lab Chip 9 (2009) 2391.
[20] R. Nielson, B. Kaehr, J.B. Shear, Small 5 (2009) 120.
[21] P. Tayalia, C. Mendonca, E. Mazur, Adv. Mater. 20 (2008) 4494.
[22] K. Takada, D. Wu, Q.D. Chen, S. Shoji, H. Xia, S. Kawata, H.B. Sun, Opt. Lett. 34 (2009) 566.
[23] L. Li, R.R. Gattass, E. Gershgoren, H. Hwang, J.T. Fourkas, Science 324 (2009) 910.
[24] H. Xia, J. Wang, Y. Tian, Q.D. Chen, X.B. Du, Y.L. Zhang, Y. He, H.B. Sun, Adv. Mater. 22 (2010) 3204.
[25] R. Guo, S. Xiao, X. Zhai, J. Li, A. Xia, W. Huang, Opt. Express 14 (2006) 810.
[26] Q.D. Chen, D. Wu, L.G. Niu, J. Wang, X.F. Lin, H. Xia, H.B. Sun, Appl. Phys. Lett. 91 (2007) 171105.
[27] M. Mizoshiri, H. Nishiyama, J. Nishii, Y. Hirata, Appl. Phys. A 98 (2010) 171.